Effects of RF Imperfections on Interference Rejection Combining Based Black-Space Cognitive Radio

Sudharsan Srinivasan, Sener Dikmese and Markku Renfors
Electrical Engineering, Faculty of Information Technology and Communication Sciences
Tampere University, Tampere, Finland
{sudharsan.srinivasan, sener.dikmese, markku.renfors}@tuni.fi

Abstract - In this paper, we investigate the effects of RF transceiver's imperfections on the multi-antenna interference rejection combing (IRC) based black-space cognitive radio (BS-CR) operation. In particular, we explore the effects of power amplifier (PA) nonlinearities and carrier frequency offset (CFO) on the blind IRC technique. The BS-CR operation mode supports effective reuse of the primary user (PU) spectrum, especially for relatively short-distance CR communication. We assume that both the PU system and the BS-CR use orthogonal frequency division multiplexing (OFDM) waveforms with common numerology. In this case the PU interference on the BS-CR signal is strictly flat-fading at subcarrier level, and it can be suppressed using subcarrier-wise IRC processing. Spatial sample covariance matrix-based IRC adaptation is applied during silent gaps in CR operation. We propose an analytical framework for modeling CFO effects, together with experimental study of CFO and PA nonlinearity effects. The performance of the IRC scheme is tested considering terrestrial digital TV broadcasting (DVB-T) as the primary service. The validity of the offered expressions for CFO effects are justified through comparisons with respective results from computer simulations. The effect of CFO between the primary and secondary systems is found to be critical for BS-CR operation, while the effect of CR transmitter's nonlinearity is no worse than in basic OFDM schemes, and the PU transmitter's nonlinearity has minor effect on BS-CR operation.

Keywords *Black-space cognitive radio, underlay CR, IRC, interference rejection combining, MRC, multi-antenna system, receiver diversity, PA nonlinearity, CFO, OFDM, DVB-T.*

I. INTRODUCTION

Spectrum reuse has become an essential part of today's wireless communication systems. Cognitive radios (CRs) are becoming a prominent means by which the spectrum reuse is implemented [1]-[3]. To operate in radio environments with a high level of interference and, simultaneously, produce negligible interference to the primary users (PUs), CR transmitters (TXs) have to have good power amplifiers (PA) that have good power efficiency and high linearity [4]. Indeed, the power efficiency and linearity requirements are conflicting. There is also the need to use the spectrum as efficiently as possible and, therefore, spectrally efficient modulation techniques such as orthogonal frequency division multiplexing (OFDM) are commonly used. OFDM systems are very sensitive to the nonlinear distortions introduced by the analogue parts. To avoid significant degradation of the signal quality, the requirements of the analogue radio frequency (RF) components, such as PA are becoming stricter [4, 5].

In this paper we study interference rejection combing (IRC) based multi-antenna receiver diversity schemes with co-channel interference rejection capability. Our focus is on the black-space cognitive radio (BS-CR) application, where the power level of the CR signal is much below the PU power level at the CR receiver, and IRC is used for co-channel interference suppression.

Linear minimum mean square error (MMSE) based multi-antenna interference cancellation of co-channel interferes was studied in [6]. The equivalence of such MMSE schemes and interference rejection combing (IRC) was described in [7]. The use of multiple adaptive antennas in the context of interference cancelation for systems based on OFDM was discussed in [8]. The effects of MMSE based IRC receiver imperfections in cellular radio systems were studied in [9].

It is important to study the effects of different kinds of RF imperfections also in the design of transceivers for CRs [4],[5],[10] and [11]. This is particularly important for black-space cognitive radio (BS-CR) operation as some of the RF imperfections may become critical due to the wide signal dynamic range in the receiver [12]-[15]. In BS-CR, the RF nonidealities may affect in two different ways: (i) Directly degrading the CR link performance and/or (ii) harming the IRC process leading to reduced PU interference suppression capability, e.g., by distorting the spatial covariance estimate. In this paper, we investigate the effects of transmitter nonlinearities and carrier frequency offset (CFO) in IRC based BS-CR systems.

In the following, we introduce first the IRC-based BS-CR system model in Section II. In Section III, the used nonlinear PA model is first introduced and then simulation results for the effects PU TX nonlinearity and target CR TX nonlinearity are presented. In Section IV, we analyze the CFO effect and develop a novel analytical model for the post-combining signal-to-interference ratio (SIR) at the CR receiver and validate the model through comparisons with simulation results. Here the post-combining SIR is the ratio of the target CR signal power at CR receiver to the residual PU interference power due to the CFO, and it is a function of the CFO in relation to the subcarrier spacing, maximum delay spread of the PU channel, and the ratio of the PU and target CR powers at the CR receiver. Finally, concluding remarks are presented in Section V.

II. IRC-BASED BLACKSPACE COGNITIVE RADIO

The scenario considered in this study is illustrated in Fig. 1. In this scenario, we consider a CR receiver using multiple antennas to receive data from a single-antenna cognitive transmitter. The CR operates within the frequency band of the PU, and the PU power spectral density (PSD) is very high in comparison to that of the CR. The PU transmitter generates a lot of interference to the CR transmission, which operates closer to the noise floor of the primary receiver, and due to this, the PU communication link is protected. We consider frequency reuse over relatively small distances, such as an indoor CR system. The multi-antenna configuration studied here is that of single-input multiple output (SIMO). Other configurations, involving also transmit diversity in the CR link are also possible, but they are left as a topic for future studies.

In the case presented in the study, the PU is a DVB-T system that uses CP-OFDM [13]-[15]. The CR system is also an OFDM based multicarrier system using the same subcarrier spacing and CP length as the primary system. Thus, it has the same overall symbol duration. The CR system is assumed to be synchronized to the primary system in frequency and in quasi-synchronous manner also in time. The CP length is assumed to be sufficient to absorb the channel delay spread

together with the residual offsets between the two systems observed at the CR receiver. Consequently, the subcarrier-level flat-fading circular convolution model for spatio-temporal channel effects applies for the target CR signal, and for the PU interference signal as well. Then the IRC process can be applied individually for each subcarrier. Since the CR receiver observes the PU signal at a very high SINR level, the synchronization task is not particularly difficult and low-complexity algorithms can be utilized. Considering short-range CR scenarios, the delay spread of the CR channel has a minor effect on the overall channel delay spread to be handled in the time alignment of the two systems. Basically, if all CR stations are synchronized to the PU, they are also synchronized with each other in quasi synchronous manner. In our earlier paper, we have investigated the effects of mobility on the BS-CR system performance [15]. Here we assume stationary operation for simplicity.

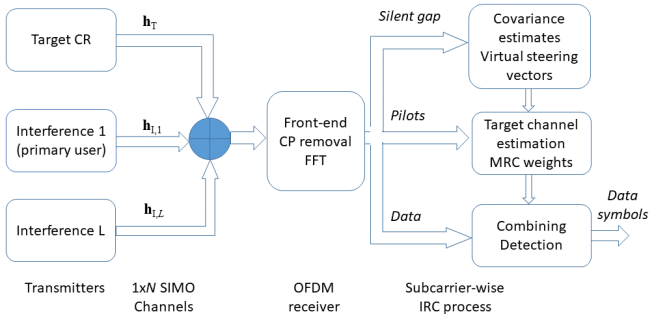

Fig. 1: BS-CR system model with silent gap for interference covariance estimation.

Both the primary and the CR systems use QAM subcarrier modulation, but usually with different modulation orders. The received CR signal consists of contributions from both the desired CR communication signal and the primary transmission signal, the latter one constituting a strong interference. Our BS-CR scheme includes two phases in the CR system operation, silent gaps and actual data transmission, as described in our previous work [15]. The spatial characteristics of the PU interference are modeled using multiantenna sample covariance matrix, which is estimated during silent gaps in the CR transmission, independently for each active subcarrier [13]. No explicit channel estimation of the PU channel is required. The CR channel is estimated from the partial IRC signals, from which the PU interference has been effectively suppressed. Based on the OFDM model mentioned above, subcarrier-wise detection is considered with flat-fading channel coefficients to get rid of the challenge of frequency selectivity in the IRC process.

In the SIMO configuration, the CR is assumed to have N receiver antennas and $L < N$ different interference sources are assumed. Based on this model, the signal received by the CR can be formulated for each active subcarrier (for simplicity of notation, the subcarrier index is not shown) as follows:

$$\mathbf{r} = \mathbf{h}_{\mathrm{T}} x_{\mathrm{T}} + \sum_{l=1}^{L} \mathbf{h}_{\mathrm{I},l} x_{\mathrm{I},l} + \boldsymbol{\eta}. \quad (1)$$

Here x_T is a transmitted subcarrier symbol and $\mathbf{h}_{\mathrm{T}} = \left[h_{\mathrm{T},1}, h_{\mathrm{T},2}, \ldots, h_{\mathrm{T},N}\right]^{\mathrm{T}}$ is the target channel vector with N receiver antennas in the CR, $x_{I,l}$ is the lth interfering signal, and $\mathbf{h}_{\mathrm{I},l} = \left[h_{\mathrm{I},l,1}, h_{\mathrm{I},l,2}, \ldots, h_{\mathrm{I},l,N}\right]^{\mathrm{T}}$ is the channel vector for the lth interferer. The channel vectors consist of the complex channel gains from the corresponding transmit antenna to nth antenna of the CR receiver. Finally, $\boldsymbol{\eta}$ is the additive white Gaussian noise (AWGN) vector. In this generic system model, it is assumed that the PU is the dominant interferer, and the other interference sources are other CR systems introducing co-channel interference at relatively low power level. The interference minimizing IRC weights are obtained during the silent period. Due to that, Eq. (1) is modified during silent gaps of CR operation as

$$\hat{\mathbf{r}} = \sum_{l=1}^{L} \mathbf{h}_{\mathrm{I},l} x_{I,l} + \boldsymbol{\eta}. \quad (2)$$

Linear combiner is used for the signals from different CR receiver antennas with a weight process in detection as follows:

$$y = \boldsymbol{w}^{\mathrm{H}} \boldsymbol{r}\,, \quad (3)$$

where y is the detected signal, $\boldsymbol{w}$ is the weight vector with N elements, and superscript H denotes the Hermitian (complex-conjugate transpose).

In this paper, we assume, for simplicity, that the PU is the only interference source. Then, if the PU channel vector is perfectly known, the noise plus interference covariance matrix can be calculated for each subcarrier as

$$\boldsymbol{\Sigma}_{\mathrm{NI}} = P\mathbf{h}_{\mathrm{I}}\mathbf{h}_{\mathrm{I}}^{\mathrm{H}} + P_N\mathbf{I}, \quad (4)$$

where P is the transmitted signal power in the subcarrier, P_N is the subcarrier noise power, and $\mathbf{I}$ is NxN identity matrix. The sample covariance based estimate is

$$\hat{\boldsymbol{\Sigma}}_{\mathrm{NI}} = \frac{1}{M} \sum_{m=1}^{M} \hat{\mathbf{r}}(m)\hat{\mathbf{r}}(m)^{H}. \quad (5)$$

Here m is the OFDM symbol index and M is the observation length in subcarrier samples, which is chosen equal to the length of the silent gap. In the following, our focus is on the sample covariance approach, but also results with known channel approach are included as a reference corresponding to ideal interference covariance estimation.

Using IRC, interference-free signals can be obtained for a transmissiom with target channel vector (known as steering vector) $\mathbf{h}_{\mathrm{S}}$ by using a linear weight vector $\mathbf{w}$ as follows:

$$\mathbf{w} = \hat{\boldsymbol{\Sigma}}_{\mathrm{NI}}^{-1}\mathbf{h}_{\mathrm{S}}. \quad (6)$$

Our approach is to calculate first such weight vectors for N orthogonal steering vectors during silent gaps and then use these weight vectors to obtain N variants of the following received CR signal block from which the PU interference is removed. Then the target CR channel is estimated for each of these signals, which are finally combined using maximum ratio combining (MRC). Details and results of these approaches can be found in our previous work [15].

III. Nonlinear PA Effects In BS-CR

A. Transmitter power amplifier models

The non-linearity of transmitter PAs causes significant effects on the performance with respect to spectrum characteristics, multiuser interference on the desired signal, and transmit power, depending on the used modulation scheme [16, 17]. Especially, the non-linearity brings about spectral regrowth causing adjacent channel interference and in-band performance degradation. The latter one is in the main focus of our study. Generally, the error vector magnitude (EVM) metric quantifies the in-band distortion causing performance loss in bit error rate (BER).

Various PA modeling approaches are available in the literature [16, 17]. While advanced PA models involving memory effects are able to model nonlinear PAs in a more reliable way, especially in wideband transmission, basic memoryless models are still widely used, e.g., in the 3GPP standardization related studies. For 5G New Radio studies at below 6 GHz frequency bands, a Rapp-type model is proposed for the base-station TX (downlink) and a polynomial model for the PAs of user devices (uplink) in [18]. Both of these gives AM/AM and AM/PM conversion characteristics, modeling how the PA output amplitude and phase, respectively, depend on the input amplitude.

Here we use the uplink model, which is an empirical polynomial model based on measurement of a real PA [18]. The PA output $y(t)$ is computed from input amplitude $x(t)$, given in dBm units, using the formula

$$y(t) = p_0 + p_1 x(t) + p_2 x(t)^2 + \cdots + p_9 \cdot x(t)^9. \quad (7)$$

The coefficients for AM/AM and AM/PM conversion, organized as $[p_9\ p_8\ p_7\ \ldots\ p_0]$ are as follows:

$$p_{\text{am}} = [\ 7.9726\text{e-}12\ \ 1.2771\text{e-}9\ \ \ 8.2526\text{e-}8\ \ 2.6615\text{e-}6\ \ 3.9727\text{e-}5\ \ 2.7715\text{e-}5\ \ \text{-}7.1100\text{e-}3\ \ \text{-}7.9183\text{e-}2\ \ \ 8.2921\text{e-}1\ \ \ 27.3535] \quad (8)$$

$$p_{\text{pm}} = [\ 9.8591\text{e-}11\ \ 1.3544\text{e-}8\ \ \ 7.2970\text{e-}7\ \ 1.8757\text{e-}5\ \ \ 1.9730\text{e-}4\ \ \text{-}7.5352\text{e-}4\ \ \text{-}3.6477\text{e-}2\ \ \text{-}2.7752\text{e-}1\ \ \text{-}1.6672\text{e-}2\ \ 79.1553]\ . \quad (9)$$

The AM/PM model gives the input amplitude dependent phase rotation in degrees.

B. PA nonlinearity effects

We test the effects of PU and CR transmitter nonlinearities through simulations. For simplicity, it is assumed that there are no other interference sources. First the spectral regrowth due to nonlinearities is demonstrated in Figs. 2 and 3 for PU TX and CR TX, respectively, for linear PA and the mentioned 5G uplink PA model. For the nonlinear model, we use two different back-off values of 9 dB (modest case) and 5 dB (worst case).

Here and in all later simulations, we assume the OFDM IFFT/FFT size of 2048 and the subcarrier spacing of 4.4643 kHz, corresponding to the 2k mode of DVB-T. The CP length is 1/8 times the main OFDM symbol duration, and the PU signal has all the elements of DVB-T transmission. For the CR signal we use the same main parameters and 1200 active subcarriers in the center of the DVB-T spectrum consisting of 1705 active subcarriers. We use the silent gap length of 24 OFDM symbols, and data block length of 65 OFDM symbols between silent gaps. We consider both sample covariance and known channel based IRC schemes. In the sample covariance based case, the covariance matrix is estimated from the received signal during silent gaps of length 24 in the target CR transmission. The reference case is based on perfect knowledge of the PU-CR channel. The CR channel is estimated using training symbols. All simulations use 1x4 SIMO antenna configuration.

Next, we consider the BER performance of the CR link with PA nonlinearity. The CR TX nonlinearity should not affect the interference covariance estimation, so we expect that it affects the BS-CR link performance in the same way as in basic OFDM transmission with the same numerology.

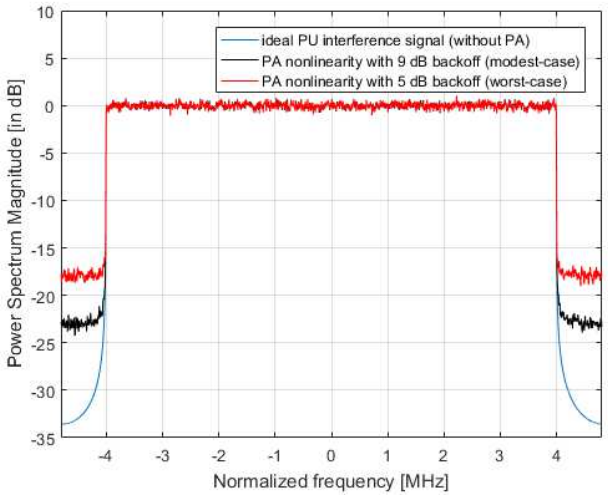

Fig. 2. Effects of PA model on PU interference signal considering ideal, modest and worst cases.

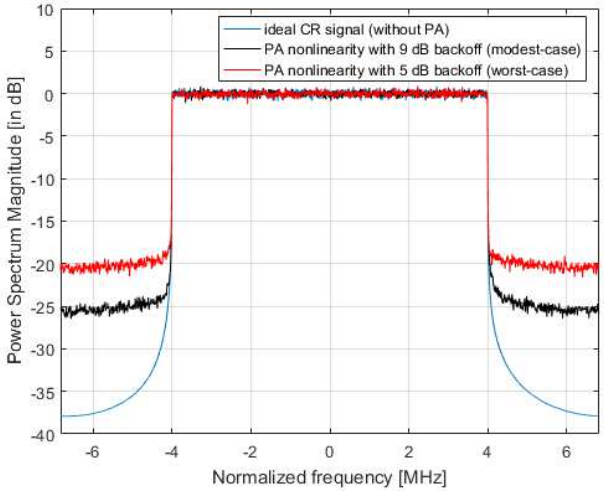

Fig. 3. Effects of PA model on CR signal considering ideal, modest and worst cases.

Regarding the PU TX nonlinearity, we notice that basic PA nonlinearity models do not harm the cyclic convolution model of CP-OFDM, i.e., the end part of the main OFDM symbol is affected in the same way as its copy, the cyclic prefix. Then the interference covariance should not be affected by PU TX nonlinearity, and we don't expect significant effects in the link performance. However, if the PA exhibits strong memory effects, the cyclic convolution model might be distorted, and this effect is worth investigating in future studies.

Monte Carlo simulation results are provided for the CR link performance with PA nonlinearity, assuming the CR/PU power ratio of $SIR_{\text{PU}} = -30$ dB and 64QAM subcarrier modulation. We use a modest input back-off value of 9 dB for the CR TX, and a low back-off value of 5 dB for the PU TX. The latter choice, as well the use of 5G-UL PA model for the PU TX is for demonstrating the robustness of BS-CR operation towards the PU TX nonlinearity. For these results, we use the Hilly terrain (HT) channel model having about 18 μs maximum delay spread for the PU signal and the ITU-R Vehicular A (VehA) model with about 2.5 μs maximum delay spread for the CR signal.

Fig. 4 shows the sample covariance based BS-CR link's BER performance with linear and nonlinear PA models in comparison to a basic interference-free link using MRC based receiver diversity. We can see that the used modest nonlinearity affects in a similar way in BS-CR and basic OFDM systems with the same numerology and same antenna configuration. With used parameters, sample covariance based BS-CR has about 3.5 dB SNR loss due to PU interference at 1 % BER level.

Fig. 5 shows the BER performance with linear/nonlinear PA in PU or CR TX, considering both sample covariance and known channel based schemes. We can see that even the very hard nonlinearity tested for PU TX has very minor effect on the CR link performance. It is also interesting to notice that, at 1 % BER level, the proposed sample covariance based method has about 1.2 dB SNR loss in comparison to the known channel based reference method.

IV. Analysis of CFO Effects in BS-CR

In the following analysis, we assume that the CR receiver is synchronized to the target CR signal while there is a frequency offset between the PU and CR carrier frequencies. We ignore the possible inconsequential initial carrier phase offset in the receiver. For convenience of notation, without loss of generality, we also assume that the active subcarriers are indexed from 0 to N_A-1. Then the PU interference part of the received digital baseband multi-antenna signal can be expressed in the presence of CFO as:

$$\boldsymbol{r}_{\mathrm{PU}}(n) = \tilde{\boldsymbol{h}}_{\mathrm{PU}}(n) * x_{\mathrm{PU}}(n) e^{\frac{j2\pi\delta_{\mathrm{CFO}} n}{N}} \tag{10}$$

where n is the time index, δ_{CFO} is the CFO normalized to the subcarrier spacing, $\tilde{\boldsymbol{h}}_{\mathrm{PU}}(n)$ is the vector of channel impulse responses from PU to the CR receiver antennas, $x_{\mathrm{PU}}(n)$ is the PU signal, and $*$ denotes cyclic convolution. Then, after the receiver's FFT process, the corresponding PU interference contributions to the kth subcarrier samples of different antenna branches can be expressed as [19]

$$\begin{aligned}\mathbf{Y}_{\mathrm{PU},k} &= \sum_{n=0}^{N-1}\left(\sum_{l=0}^{N_A-1}\mathbf{h}_{\mathrm{PU},l} d_{\mathrm{PU},l} e^{j2\pi ln/N} e^{j2\pi\delta_{\mathrm{CFO}} n/N}\right) e^{-j2\pi kn/N} \\ &= \sum_{l=0}^{N_A-1}\mathbf{h}_{\mathrm{PU},l} d_{\mathrm{PU},l} \sum_{n=0}^{N-1} e^{j2\pi(l-k+\delta_{\mathrm{CFO}})n/N} \\ &= \sum_{l=0}^{N_A-1}\phi(l-k+\delta_{\mathrm{CFO}})\beta(l-k+\delta_{\mathrm{CFO}})\mathbf{h}_{\mathrm{PU},l} d_{\mathrm{PU},l}\end{aligned} \tag{11}$$

where $\boldsymbol{h}_{\mathrm{PU},l}$ is the PU channel vector for subcarrier l, $d_{\mathrm{PU},l}$ is the PU data symbol in subcarrier l, and

$$\begin{aligned}\phi(z) &= e^{j\pi z(N-1)/N} \\ \beta(z) &= \frac{\sin(\pi z)}{N\sin(\pi z/N)},\end{aligned} \tag{12}$$

with $z = l-k+\delta_{\mathrm{CFO}}$. The orthogonality of subcarriers is maintained only if the CFO is zero or integer, i.e., if the frequency offset is an integer multiple of subcarrier spacing. Otherwise, the sample observed at the kth subcarrier contains intercarrier interference (ICI) from all other active subcarriers.

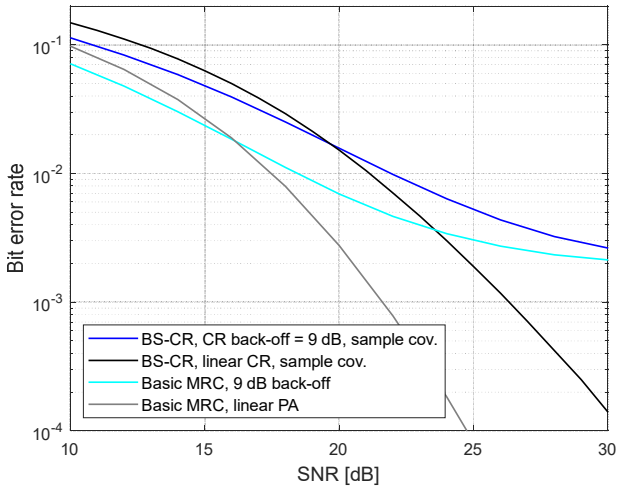

Fig. 4. BER performance of sample covariance based BS-CR with 64QAM modulation and $SIR_{\mathrm{PU}} = -30$ dB vs. basic transmission link with MRC based receiver diversity. 5G-UL PA model is used for the target link, linear PA in PU TX.

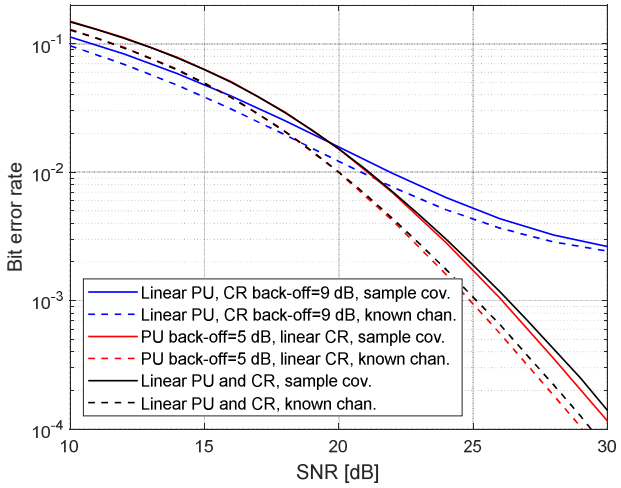

Fig. 5: BER performance of BS-CR with 64QAM subcarrier modulation, $SIR_{\mathrm{PU}} = -30$ dB, and linear or nonlinear 5G-UL PA model for PU or CR transmitter.

Now the known PU channel based spatial covariance matrix for subcarrier k can be evaluated as

$$\begin{aligned}\tilde{\boldsymbol{\Sigma}}_{\mathrm{PU},k} &= \left(\sum_{l=0}^{N_A-1}\phi(z)\beta(z)\mathbf{h}_{\mathrm{PU},l}\right)\left(\sum_{l=0}^{N_A-1}\phi(z)\beta(z)\mathbf{h}_{\mathrm{PU},l}\right)^{\mathrm{H}} \\ &= \sum_{l=0}^{N_A-1}\phi(z)\beta(z)\mathbf{h}_{\mathrm{PU},l}\left(\phi(z)\beta(z)\mathbf{h}_{\mathrm{PU},l}\right)^{\mathrm{H}} \\ &= \sum_{l=0}^{N_A-1}\beta^2(l-k+\delta_{\mathrm{CFO}})\boldsymbol{\Sigma}_{\mathrm{PU},l},\end{aligned} \tag{13}$$

where $\boldsymbol{\Sigma}_{\mathrm{PU},l}$ is the spatial covariance matrix of subcarrier l in the absence of CFO. The cross-terms between different subcarriers are not included here, based on the common assumption that the subcarrier symbol sequences are uncorrelated.

In the following, we aim to model the effect of CFO on the interference covariance matrix in the IRC context using basic parameters of the channel model. For this purpose, we first introduce a model for the correlation of the spatial channels of different subcarriers. We use the model commonly applied in Wiener filtering based channel estimation [20] for the correlation between the channel coefficients of different subcarriers. It is based on assuming uniform power delay profile with maximum delay spread of τ_{max}. We also assume that the spatial channel of each subcarrier is uncorrelated. Then the correlation between subcarriers k and l can be expressed as [20]

$$R(k,l) = \mathrm{sinc}\left((k-l)\tau_{\max} f_S / N\right) e^{-j(k-l)\tau_{\max} f_s / N}. \quad (14)$$

It should be noted that in case of flat-fading channel, different subcarriers have equal channel matrices and, consequently, equal spatial covariance matrices. In this case, CFO affects the channel covariance matrices on by an inconsequential real scaling factor. On the contrary, with highly frequency selective channels, the spatial covariance matrix of each subcarrier is distorted by the uncorrelated parts of the channel vectors of other subcarriers. Noting that $R(k,k) = 1$, we can express the spatial covariance matrix of subcarrier k as

$$\tilde{\boldsymbol{\Sigma}}_{\mathrm{PU},k} = \beta^2(\delta_{\mathrm{CFO}})\boldsymbol{\Sigma}_{\mathrm{PU},k} + \sum_{\substack{l=0 \\ l\neq k}}^{N_A-1} (1-R(k,l))^2 \beta^2(l-k+\delta_{\mathrm{CFO}})\boldsymbol{\Sigma}_{\mathrm{PU},l}. \quad (15)$$

The actual spatial covariance matrix of each subcarrier is scaled by $\beta^2(\delta_{\mathrm{CFO}})$, while the distorting uncorrelated part of the covariance of subcarrier k is given by the latter term. We assume that the IRC process suppresses completely the PU interference power corresponding to the first term, but the uncorrelated part remains as interference to the target CR signal. Let $SIR_{\mathrm{PU}} = P_{\mathrm{T}} / P_{\mathrm{PU}}$ denote the ratio of the target CR power at the CR receiver, P_{T}, to the PU interference power before interference cancellation, P_{PU}. Assuming that the subcarriers have equal power levels, the target signal's post-combining SIR due to the CFO of the PU signal can be evaluated as:

$$SIR_{\mathrm{CFO}}(\delta_{\mathrm{CFO}}) = \frac{SIR_{\mathrm{PU}}}{\sum_{\substack{l=0 \\ l\neq k}}^{N_A-1} (1-R(k,l))^2 \beta^2(l-k+\delta_{\mathrm{CFO}})}. \quad (16)$$

In the numerical results, we show the average of this expression over active subcarriers. This calculation can be simplified by noting that subcarriers $k+\kappa$ and $k-\kappa$ contribute equally to the interference and that, considering all active subcarriers, there are $2(N_A-\kappa)$ subcarriers at the distance of $|l-k| = \kappa$.

Fig. 6 compares the theoretical SIR values based on Eq. (16) with simulated SIR values considering both sample covariance based and known channel -based IRC schemes with different values of CFO. Here the known channel reference case is based on perfect knowledge of the PU channel in the absence of CFO. The subcarrier modulation is 16QAM, and the other parameters are as mentioned in Section III-B.

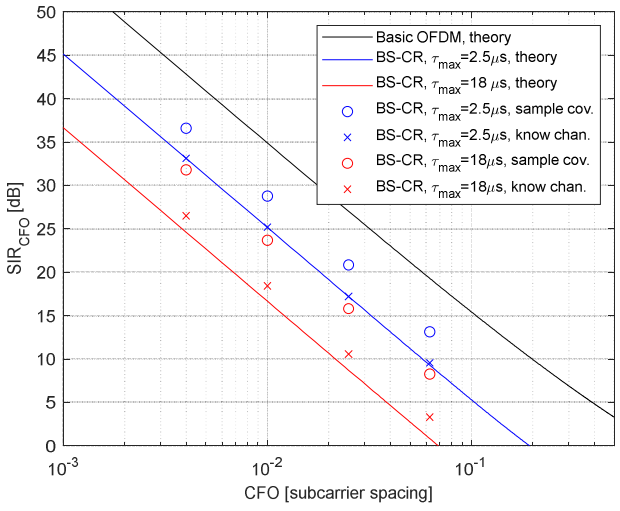

Fig. 6. Theoretical and experimental CFO-based SIR in BS-CR with Vehicular-A and Hilly terrain channel models and SIR_{PU} = -30 dB.

Here both HT and VehA channels are considered for the PU signal. No channel noise is included in these simulations, so the interference is due to imperfect spatial covariance matrix estimation due to CFO and due to limitations of sample covariance based estimation in the corresponding case. The CFO-based SIR is shown also for the basic OFDM scheme [19].

We can see that the CFO requirements are 3-10 times tighter than in basic OFDM schemes, depending on the channel delay spread and covariance estimation scheme. We can see that with the VehA-type PU channel, there is a very good match between the theoretical model and the known channel based simulation results. With HT-type PU channel, the theoretical model is somewhat pessimistic. We can also see that the sample covariance based estimation gives clearly better SIR than the theoretical model or the case of CFO-free channel knowledge based covariance estimation. This is because the sample covariance based estimation is able to take into account the CFO-induced contribution to the covariance estimates of different subcarriers.

Fig. 7 shows the BER performance with 64QAM modulation, VehA channel for the CR link, and CFO values of $\delta_{\mathrm{CFO}} \in \{0,\ 0.01, 0.005\}$, while the other parameters are the same as in the other numerical results. We can see that with CFO=0, the PU channel's delay spread has a very minor effect on the performance. When relating these results with SIR performance of Fig. 6, it should be noted for Fig. 6, the interference covariance is estimated in the absence of channel noise, and in low SNR region of Fig. 7, the covariance estimate is degraded due to noise. However, we can see that in the high SNR region, the performance of sample covariance -based scheme may exceed the performance of the known channel -based covariance estimate. Generally, the hard requirements for CFO can be seen also in these results.

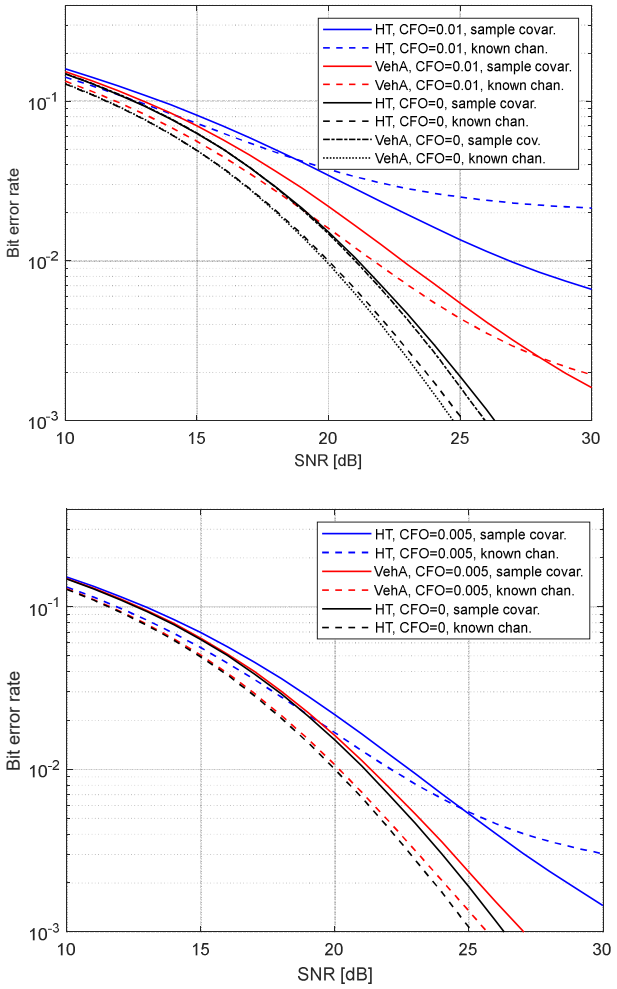

Fig. 7. BER performance with different CFO values {0, 0.005, 0.01}, 64QAM subcarrier modulation, SIR_{PU} = -30 dB, VehA channel for CR link, and VehA or HT channel for PU.

V. Concluding Remarks

Clearly, the most critical one among the considered RF imperfections is the CFO between the PU signal and CR receiver. However, since the PU signal is received at a high power level, synchronizing the CR stations to the PU signal with the needed high accuracy should be achievable. Considering other cases, e.g., when both the PU signal and target CR signal have CFOs, the effect of the high-powered PU signal dominates and still remains the most critical issue. The effects of PA nonlinearity in PU and CR transmitters were also tested, and found to less critical, as expected. The developed analytical model for the PU CFO effect could be a basis for analytical modeling BS-CR scenarios with mobility, which was tested experimentally in our earlier work in [15]. This is an important topic for future studies. Also, the nonlinearity of the CR receiver electronics may be critical due to the wide signal power range to be dealt with. This remains as another important topic for future work.

References

[1] T. Yucek and H. Arslan, "A Survey of Spectrum Sensing Algorithms for Cognitive Radio Applications," *IEEE Comm. Surveys & Tutorials*, vol. 11, no. 1, pp. 116-129, 2009.

[2] H. Viswanathan and P.E. Mogensen, "Communications in the 6G Era," *IEEE Access*, vol. 8, pp. 57063-57074, March 2020.

[3] A. M. Wyglinski et al, *Cognitive Radio Communications and Networks: Principles and Practice*, Academic Press, 2010.

[4] S. Dikmese, S. Srinivasan, M. Shaat, F. Bader and M. Renfors, "Spectrum Sensing and Resource Allocation for Multicarrier Cognitive Radio Systems under Interference and Power constraints," *EURASIP J. on Adv. in Signal Proc.,* 2014:68.

[5] M. Majidi, A. Mohammadi and A. Abdipour, "Analysis of the Power Amplifier Nonlinearity on the Power Allocation in Cognitive Radio Networks," *IEEE Trans. Comm.*, vol. 62, no. 2, pp. 467-477, Feb. 2014

[6] J. H. Winters, "Optimum Combining in Digital Mobile Radio with Co-channel Interference," *IEEE J. Select Areas Commun*., vol. SAC-2, pp.528-539, July 1984

[7] Z. Bai et al., "On the Equivalence of MMSE and IRC Receiver in MU-MIMO Systems," *IEEE Communications Letters*, vol. 15, no. 12, pp. 1288-1290, December 2011

[8] Ye Li and N. R. Sollenberger, "Adaptive Antenna Arrays for OFDM Systems with Cochannel Interference," *IEEE Trans. Comm.*, vol. 47, no. 2, pp. 217-229, Feb. 1999.

[9] F. M. L. Tavares, G. Berardinelli, N. H. Mahmood, T. B. Sorensen and P. Mogensen, "On the Impact of Receiver Imperfections on the MMSE-IRC Receiver Performance in 5G Networks," *in Proc. 2014 IEEE 79th Vehicular Technology Conference (VTC Spring)*, , pp. 1-6

[10] S. J. Heinen and R. Wunderlich, "High Dynamic Range RF Frontends from Multiband Multi Standard to Cognitive Radio," in *Proc. IEEE Semiconductor Con*. , pp. 1-8, Sep. 2011.

[11] D. Cabric, S. M. Mishra, and R. W. Brodersen, "Implementation Issues in Spectrum Sensing for Cognitive Radios," in *Signals, Systems and Computers Conference Record of the Thirty Eighth Asilomar*, vol.1, pp. 772-776, Nov. 2004.

[12] H. Zamat and B. Natarajan, "Use of Dedicated Broadband Sensing Receiver in Cognitive Radio,"in *Proc. IEEE Communications Workshop*, pp. 508-512, May 2008.

[13] Y. Selén, R. Baldemair and J. Sachs, "A Short Feasibility Study of a Cognitive TV Black Space System," in *Proc. IEEE PIMRC 2011*, pp. 520-524.

[14] S. Srinivasan and M. Renfors "Interference Rejection Combining for Black-space Cognitive Radio Communications", in *Proc. Crowncom 2018*, pp. 200-210, Sept. 2018.

[15] S. Srinivasan, S. Dikmese and M. Renfors "Enhanced Interpolation-based Interference Rejection Combining for Black-space Cognitive Radio in Time-varying Channels," *J. Wireless Com. Network* 2020, 238 (2020).

[16] K. Hyunchul and J.S. Kenney, "Behavioral Modelling of Nonlinear RF Power Amplifiers Considering Memory Effects," *IEEE Trans. Microw. Theory Tech.,* 2003, vol. 51, pp. 2495-2504, Dec 2003.

[17] G. Zhou and R. Raich, "Spectral Analysis of Polynomial Nonlinearity with Applications to RF Power Amplifiers," *EURASIP J. on Applied Signal Proc.*, pp 1831-1840, Dec 2004.

[18] R4-163314, "Realistic Power Amplifier Model for the New Radio Evaluation," Nokia, 3GPP RAN79.

[19] J. Armstrong, "Analysis of New and Existing Methods of Reducing Intercarrier Interference Due to Carrier Frequency Offset in OFDM," *IEEE Trans. Comm.*, vol. 47, no. 3, pp. 365-369, March 1999.

[20] P. Hoeher, S. Kaiser and P. Robertson, "Two-dimensional Pilot-symbol-aided Channel Estimation by Wiener Filtering," in *Proc. IEEE Int. Conf. on Acoustics, Speech, and Signal Processing*, 1997, pp. 1845-1848 vol.3.